Dynamic Strain Aging During Creep of α-Zr

R. D. WARDA, V. FIDLERIS, AND E. TEGHTSOONIAN

In the temperature range 723 to 823 K (450° to 550°C) annealed, crystal bar α-Zr exhibits anomalous behavior with respect to both single stress and incrementally stressed creep tests. The nature and extent of the anomalous behavior depends on temperature, stress, and impurity content. Specimens with low oxygen content exhibit: 1) normal, three-stage creep behavior during single stress tests, and 2) normal transients during incremental stress and temperature tests. Specimens with higher oxygen contents exhibit: 1) multi-stage creep curves whose shapes depend on temperature and stress, 2) inverse transients following stress and temperature increments, and 3) peaks in activation energy-temperature curves. The nature of the anomalous behavior is consistent with a model for strain aging in which the possibility of localized depletion of the strain aging species exists. In the material being studied oxygen is probably responsible for the observed effects.

DYNAMIC strain aging results from the interaction of dislocations and solute atoms during testing under certain conditions of strain rate and temperature. The most common manifestations of this phenomenon are serrated yielding (Portevin-Le Chatelier Effect) and anomalies in both strain rate sensitivity and work hardening during tensile testing. Certain aspects of anomalous creep behavior have also been attributed to dynamic strain aging.

The influence of dynamic strain aging on the behavior of iron and mild steels is well documented.[1-5] Certain substitutional fcc alloys such as α-brass, tin-bronze, and Al-Mg also exhibit strain aging characteristics.[6-11] In hcp materials there is evidence of weak strain aging resulting from the interaction of interstitial atoms and dislocations.[12] Commercial purity polycrystalline α-Ti exhibits serrated stress strain curves,[13,14] a peak in creep strength at intermediate temperatures,[15] and incubation creep,[16] all of which are attributable to strain aging. Serrated yielding[17] and other manifestations of dynamic strain aging such as anomalous work hardening[18] have been observed in polycrystalline Zr-O alloys. The creep behavior of Zircaloy-2 is also influenced by a strain aging reaction.[19]

This paper describes the influence of dynamic strain aging on the creep behavior of crystal bar zirconium in the temperature range 723 K (450°C) to 823 K (550°C).

EXPERIMENTAL

The material used in this investigation was crystal bar zirconium supplied in three batches by Wah Chang Corp., Albany, Oregon. The concentration ranges of the major impurities, from the supplier's certified analysis, are shown in Table I. The average oxygen concentration in each batch, determined by the neutron activation method, is also shown.

The as-received material was in the form of 2.29 mm (0.090 in.) sheet and 95.3 mm (0.375 in.) diam rod. Both the sheet and rod were cold reduced by 50 pct and machined into specimens with gauge length 2.54 cm (1 in.) and gage area 6.46 mm^2 (10^{-2} in.^{2}). After chemical polishing in a solution of 10 pct HF, 45 pct HNO_3, and 45 pct H_2O, most specimens were annealed in a vacuum of less than 5×10^{-6} torr to produce a grain size of 50 μm. Other grain sizes studied were 12 and 300 μm. After annealing the specimens were repolished and examined in a texture goniometer. All specimens exhibited the expected rolling or wire drawing textures. All tests were conducted on longitudinal specimens.

Tests were performed in vacua less than 3×10^{-6} torr in creep machines equipped with Andrade-Chalmers type constant stress lever arms. Load transmission was accomplished through a counterbalanced bellows assembly. Strain was measured with a Daytronic transducer system with a sensitivity of 1×10^{-6}. Creep curve shapes and creep rates were obtained from single stress, single temperature tests; incubation creep behavior and apparent activation energies were determined using incremental stress and temperature changes.

Microstructures of annealed and deformed specimens were examined using both optical and electron microscopy. Dislocation densities were measured by the random line intercept method[20] in foils tilted to maximize the number of visible dislocations. The foil thickness was assumed to be 2000Å. It was considered that the subsequent comparative treatment of the dislocation density results did not warrant thickness calculation for all foils.

RESULTS

General Behavior

Creep rates and creep curve shapes were reproducible only within batches A and C. Batch B exhibited

Table I. Concentration of Major Impurities in wt ppm

Impurity	Supplier's Analysis, Range for 3 Batches	Neutron Activation Analysis		
		Batch A	Batch B	Batch C
O	50 to 150	22	45	65
N	5 to 50			
Fe	50 to 200			
all others	100			

R. D. WARDA, formerly of Department of Metallurgy, University of British Columbia, is now with Mines Branch, Department of Energy, Mines, and Resources, Ottawa, Canada. V. FIDLERIS is with Fuels and Materials Division, Chalk River Nuclear Laboratories, Chalk River, Ontario, Canada. E. TEGHTSOONIAN is with Department of Metallurgy, University of British Columbia, Vancouver, British Columbia, Canada.

Manuscript submitted June 5, 1972.

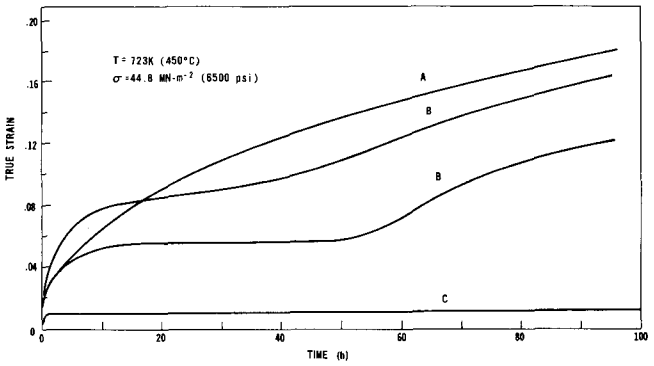

Fig. 1—Creep curves of batches A, B, and C at 723 K (450°C) and 44.8 MN·m^{-2} (6500 psi).

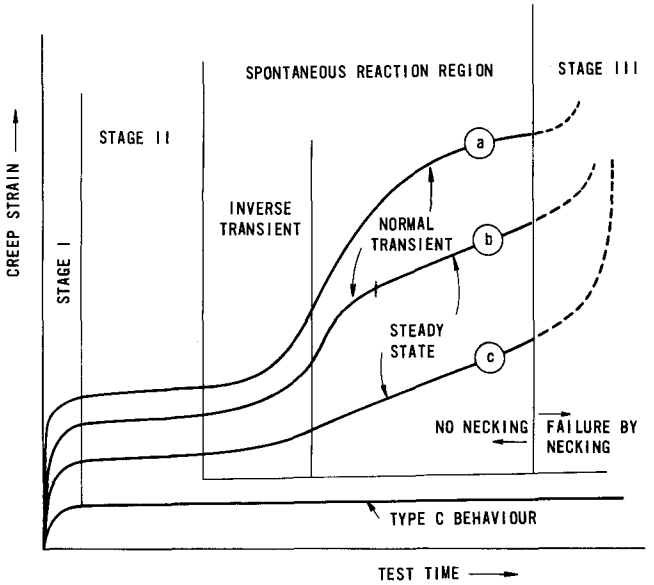

Fig. 2—Schematic illustration of batch B and C material creep behavior.

a spectrum of behavior, the limits of which were delineated by the other two batches.

Fig. 1 illustrates the various types of creep curve (A, B, and C) obtained by testing specimens from the respective batches at 723 K (450°C) and 44.8 MN·m^{-2} (6500 psi). Type A, or "normal" creep behavior, is similar to that exhibited by other pure, polycrystalline materials at similar homologous temperatures. Type B and C, or "anomalous" behavior, summarized schematically in Fig. 2, is characterized by a shorter stage I, a lower creep rate in stage II, followed, under certain conditions, by an inverse transient (period of increasing creep rate) which is terminated by either: a) a normal transient (period of decreasing creep rate), b) a normal transient followed by a new steady state, or c) a new steady state. The occurrence, under constant test conditions, of an inverse transient, followed by either (a), (b), or (c) will be referred to subsequently as a *"spontaneous" reaction*. The major differences between type B and type C behavior are in the degree of departure from normal behavior and in the absolute creep rates. Type C specimens exhibit more pronounced behavioral anomalies and the lowest steady state creep rates. Spontaneous reactions in type C specimens occur rarely and only after extensive periods of steady state creep.

Effect of Temperature

The behavior of batch A specimens was the same throughout the temperature range studied. For batch B and C specimens at 723 K (450°C) spontaneous reactions involved characteristics (a) or (b), Fig. 2; at 773 K (500°C) and 823 K (550°C), inverse transients were followed by characteristics (b) or (c).

Effect of Stress

Batch A specimens showed normal variation of behavior with stress. At low and intermediate stresses, all three creep stages were observed; at high stresses, specimens passed directly from primary to tertiary creep.

The influence of stress on the behavior of samples from batches B and C was more complicated. The influence of stress on the behavior of batch B at 773 K (500°C) and batch C at 723 K (450°C) is illustrated in Figs. 3 and 4, respectively. At low stresses only type C behavior is observed. At intermediate stresses, both batches exhibited type B behavior, with the spontaneous reaction occurring at lower stresses and strains in batch B samples. At high stresses, only type A behavior was exhibited.

Steady State Creep Rates

The abnormal behavior exhibited by specimens from batches B and C complicates the presentation of steady state creep data. Under certain conditions, the early occurrence of a spontaneous reaction precluded the measurement of prereaction steady state rates. For specimens tested under conditions such that steady creep both preceded and followed spontaneous reactions, both rates are plotted, with open and filled symbols representing pre- and postreaction behavior, respectively. The symbol S is used to connect corresponding pre- and postreaction steady state creep rates.

Figs. 5, 6, and 7 illustrate the behavior of all the materials tested at 723 K (450°C), 773 K (500°C), and 823 K (550°C). At all temperatures prereaction creep rates of batch B and C specimens were more than one order of magnitude lower than those of batch A. Postreaction creep rates were similar to those of batch A

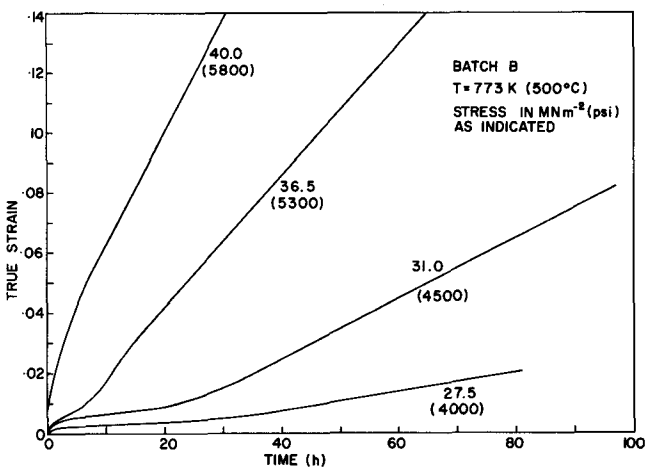

Fig. 3—Influence of stress on creep curves of batch B material at 773 K (500°C).

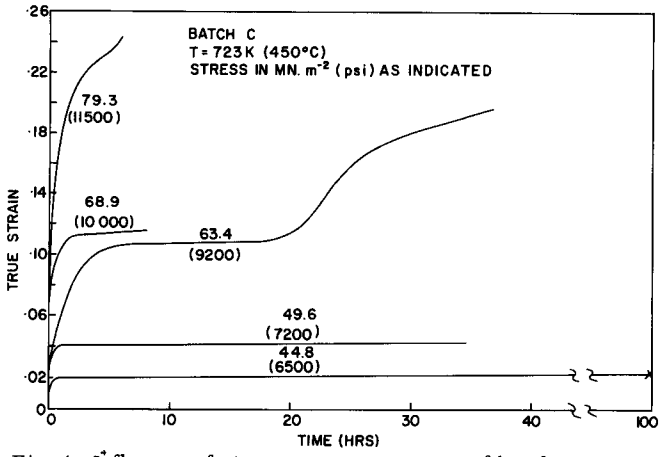

Fig. 4—Influence of stress on creep curves of batch C material at 723 K (450°C).

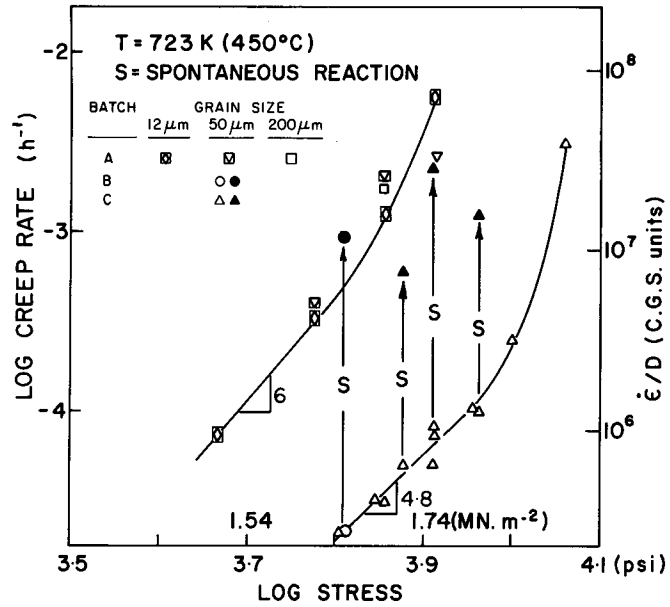

Fig. 5—Relationship between stress and steady state creep rate or diffusion compensated creep rate ($\dot{\epsilon}/D$) at 723 K (450°C), where D = bulk diffusion of oxygen in α-Zr.

at 723 K (450°C), but were lower at the higher temperatures.

The effect of grain size on steady state creep rate was investigated for batch A material at 723 K (450°C) and 773 K (500°C) only. The grain sizes used were 12, 50, and 300 μm. From the results in Figs. 5 and 6 it would appear that the effect of grain size on steady state creep is small and varies with stress, suggesting a transition from slip dominated to grain boundary dominated behavior.

Stress Increment Tests

The response of specimens to stress increments will be described as "induced" reactions, the three types of which are described schematically in Fig. 8. Normal induced reactions occurred under all conditions for batch A samples, but only from increments applied subsequent to a spontaneous reaction for batches B and C. Increments applied prior to spontaneous reactions caused abnormal induced reactions in batch B specimens and incubation induced reactions in batch C.

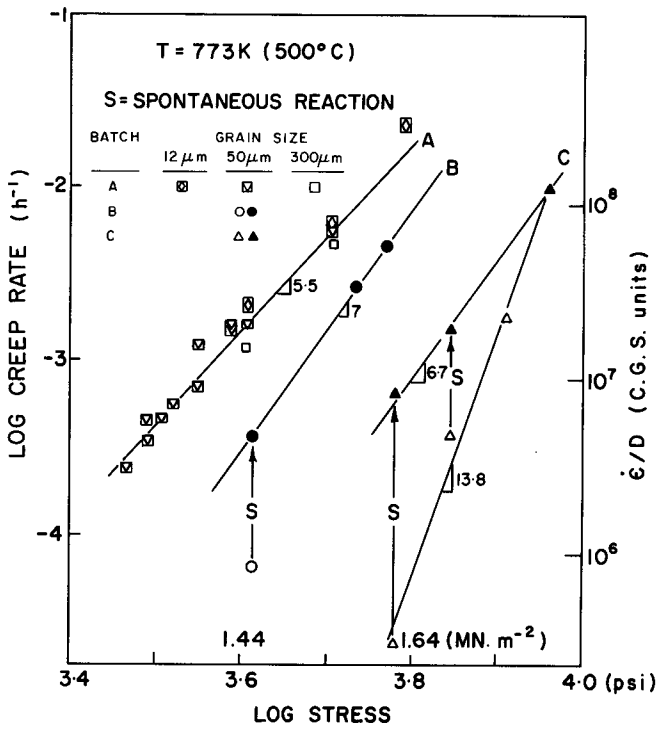

Fig. 6—Relationship between stress and steady state creep rate or diffusion compensated creep rate ($\dot{\epsilon}/D$) at 773 K (500°C), where D = bulk diffusion of oxygen in α-Zr.

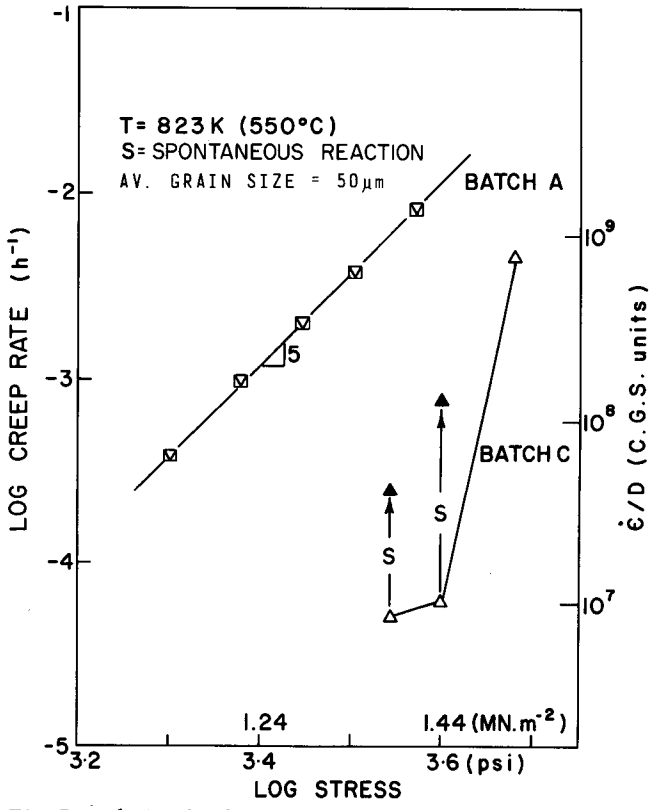

Fig. 7—Relationship between stress and steady state creep rate or diffusion compensated creep rate ($\dot{\epsilon}/D$) at 823 K (550°C), where D = bulk diffusion of oxygen in α-Zr.

Temperature Increment Tests

Temperature increment tests were performed in the range 300 to 885 K (27° to 612°C) to determine the apparent activation energy for creep in this region. The

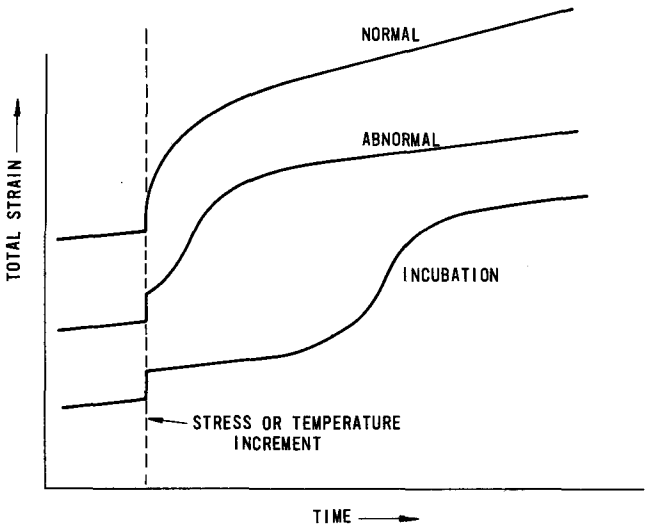

Fig. 8—Schematic illustration of creep rate transients following a perturbation.

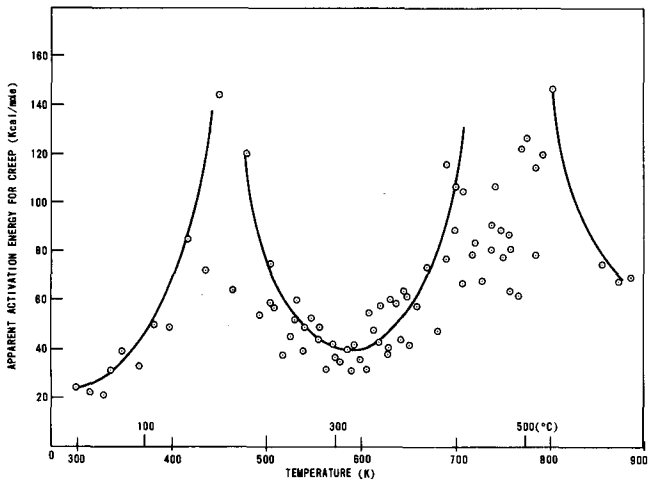

Fig. 9—Relationship between apparent activation energy for creep and temperature.

strain rates were measured as closely as possible to the increment in an attempt to approach the isostructural requirement.

Fig. 9 illustrates that there are two peaks in the activation energy, one in the temperature range 673 to 823 K (400° to 550°C), and one at 423 to 473 K (150° to 200°C).

Metallography

Examination of surface deformation characteristics suggests that certain aspects of the abnormal creep behavior exhibited by specimens from batches B and C are related to changes in slip distribution. Prior to a spontaneous reaction, slip is uniformly distributed across the grains. During and subsequent to the reaction, however, deformation occurs by the intensification of certain slip bands, as illustrated in Fig. 10. Bands of intense slip in individual grains nucleate similar bands in adjacent grains, establishing networks of concentrated deformation. No evidence of recrystallization or necking was detected in the numerous samples in which spontaneous reactions occurred.

After annealing all three materials consisted of

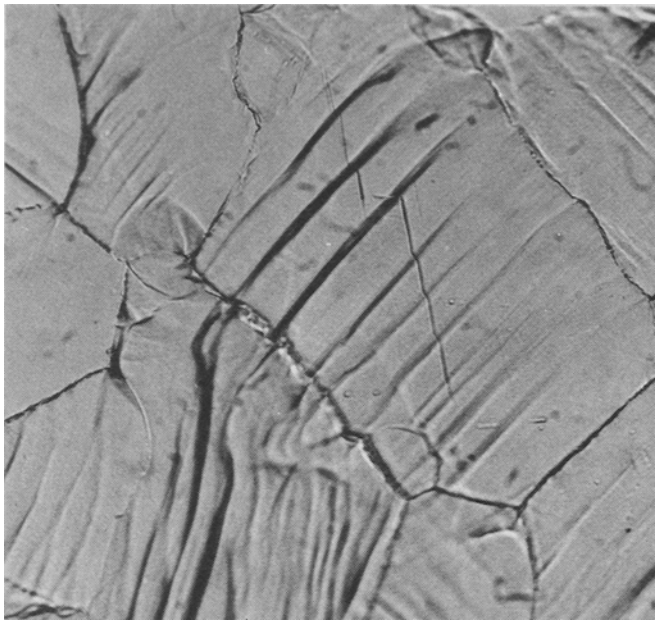

Fig. 10—Example of slip band intensification. Magnification 500 times.

grains in which no substructure was evident with an average dislocation density of 2×10^{7} cm^{-2}. However, when deformed under identical conditions, different dislocation arrangements and densities were observed, as shown in Table II.

DISCUSSION

Results obtained during this investigation have shown that polycrystalline, crystal bar α-Zr creep specimens obtained from three batches of similar material and with identical, annealed microstructures can exhibit significantly different creep behavior and microstructures when deformed under identical conditions of stress and temperature. There appears to be a correlation between the behavioral and microstructural variations and the oxygen content of the three batches. Batch A, with the lowest oxygen content, exhibited normal, reproducible creep behavior, Fig. 1, under conditions of constant stress and temperature, and normal responses to stress increments. Batches B and C exhibited variable, anomalous behavior under constant creep conditions and anomalous responses to stress increments. The degree of departure from the normal (type A) behavior increased with oxygen content.

The creep behavior exhibited by batches B and C is similar to the anomalous behavior observed in α-Fe,[1,3] α-Ti,[21] α-brass,[22] and Al-Mg[23] alloys in which the anomalies have been attributed to dynamic strain aging. Behavioral anomalies shared by batches B and C and this group of strain aging materials are:

—a rapid decrease in the initial creep rate followed by a low steady state creep rate,

—induced abnormal and incubation reactions,

—maxima in apparent activation energy.

The correlation between the appearance of the strain aging characteristics in the three batches and their respective oxygen contents, Table I, suggests that oxygen is the impurity responsible for the strain aging reaction. Further support for this suggestion is obtained from the application of Cottrell's atmosphere drag

Table II. Dislocation Densities and Grain Sizes of Creep Specimens Tested at 723 K (450°C) and 56.5 MN·m^{-2} (8200 psi)

Material	Before Creep Test		Creep Strain	Creep Rate, h^{-1}	After Creep Test		
	Dislocation Density,* cm^{-2}	Grain Size, μm			Dislocation Density,* cm^{-2}	Grain Size, μm	Subgrain Size, μm
batch A	2×10^7	50	0.14	4.8×10^{-3}	9×10^8	50	4 to 6
batch C before spontaneous reaction	2×10^7	50	0.08	7×10^{-5}	7×10^8	50	(50)
batch C after spontaneous reaction	2×10^7	50	0.14	2.4×10^{-3}	2×10^9	50	4 to 6

*Dislocation densities based on measurements of 10 or more plates of magnification 10 K.

model[24] in which the creep rate and diffusion rate of the strain aging solute are related by the expression

$$\frac{\dot{\epsilon}}{D} \leq 10^7 \text{ (in cgs units)} \quad [1]$$

Using Pemsler's results[25] for the bulk diffusion of oxygen in α-Zr, the calculated ratio of $\dot{\epsilon}/D$ is plotted on the right hand side of Figs. 5, 6, and 7. At all three temperatures, the creep rates for batches B and C measured prior to the occurrence of spontaneous reactions satisfy Eq. [1].

However, Cottrell's dynamic strain aging model does not explain all aspects of the observed anomalous behavior. The occurrence of spontaneous reactions and the resultant changes in both creep behavior and microstructure require a modification of the strain aging mechanism.

Spontaneous reactions occur at lower stresses and strains in batch B than in batch C specimens. Spontaneous reactions are also accompanied by:

—an increase in steady state creep rate of more than one order of magnitude

—an increase in dislocation density and the formation of subgrains

—slip band intensification,

—a transition in response to stress increments from anomalous to normal.

The appearance of spontaneous reactions in batches B and C, and the resultant behavioral and microstructural transitions can be understood if it is assumed that these phenomena are manifestations of a sudden decrease in strain aging capacity during steady state creep resulting from a localized depletion of solute atoms. The diffusion of solute atoms in the stress field of a dislocation[24,26] and the recurring motion of dislocations in an active slip band would have the effect of sweeping out the solute atoms in the vicinity of the band. The result of solute depletion will be a decrease in the solute drag component of the internal stress and a corresponding increase in dislocation velocity under conditions of constant structure, applied stress, and temperature. The increase in dislocation velocity resulting from depletion will be sufficient to preclude further solute atom interaction and the solute atom drag stress vanishes, compounding the increase in dislocation velocity. The external manifestation of such a phenomenon would be an inverse transient. Dislocation multiplication during the inverse transient would result in an increase in the structure-sensitive component of the internal stress,[27] causing the velocity of the dislocations to decrease. Such a process manifests itself as a normal transient in the creep curve. As the velocity of the dislocations decreases, the probability of interaction with solute atoms increases. However, the maximum drag stress is now relatively low, commensurate with the locally reduced solute concentration, and in subsequent deformation the solute drag stress plays a relatively minor role.

Phenomena attributed to solute depletion have been observed in iron containing 40 ppm by weight dissolved nitrogen.[28] The low impurity levels of our materials make solute depletion a possibility. This hypothesis is also supported by the correlation between the order of appearance of spontaneous reactions in the three batches of material and their oxygen contents.

In batch A material effective depletion probably occurs early in stage I creep. At a given stress and temperature spontaneous reactions occur earlier in batch B than in batch C, since less stress-directed diffusion is required to achieve a critical level of localized depletion in the material with the lower initial oxygen content.

The increase in creep rate after the spontaneous reaction is associated with higher dislocation densities and the formation of subgrains, Table II, *i.e.*, higher internal structural stress. These observations appear to contradict the results of other investigators.[27,29] However, the contradiction is resolved by the solute depletion hypothesis. The spontaneous reaction indicates the loss of the solute drag component and an increase in the structural component of the internal stress. This increase in the structural stress is confirmed not only by an increase in the dislocation density, and the formation of subgrains, but also by the presence of a normal transient in the creep curve. The increase in the creep rate, in spite of the increase in internal stress, indicates the importance of the solute drag component of the internal stress prior to depletion.

Slip band intensification is also a manifestation of the transient nature of the solute atom drag stress. As a result of depletion, active slip bands become softer than the surrounding crystal, and slip will concentrate in these bands until an increase in the structural internal stress compensates for the absence of the drag stress.

Induced abnormal and incubation reactions result from the creation of "free" dislocations by the perturbation of a strain aging material.[3] A spontaneous reaction is accompanied by a transition in response to increments from abnormal to normal. This transition

is in complete agreement with the suggestion that the spontaneous reaction signifies a loss of strain aging capacity.

The observation of abnormal reactions after temperature increments also implies the creation of free dislocations. This not only invalidates the isostructural criterion of the incremental test, but also changes the structure in a way which would yield a higher activation energy. Therefore, the presence of the peak in the apparent activation energy is considered to be an indication of strain aging rather than a quantitative measurement of the activation of the aging process.

CONCLUSIONS

α-Zr exhibits anomalous creep behavior in the temperature range 723 to 823 K (450° to 550°C). The anomalies consist of abnormal responses to stress increments, spontaneous changes in creep rate, activation energy maxima, and slip band intensification. This behavior is consistent with a dynamic strain aging model in which the possibility of solute depletion exists. A correlation between oxygen content and the strength and duration of the aging effect supports the model and suggests that oxygen is the species responsible.

ACKNOWLEDGMENTS

Two of the authors (R.D.W. and E.T.) gratefully acknowledge support of this work through a research grant from Atomic Energy of Canada Limited.

REFERENCES

1. M. Gensamer and R. F. Mehl: *AIME Trans.*, 1938, vol. 131, p. 372.
2. M. J. Manjoine: *J. Appl. Mech.*, 1944, vol. 11, p. A211.
3. R. J. Arsenault and J. Weertman: *Acta Met.*, 1963, vol. 11, p. 1119.
4. D. J. Dingley and D. McLean: *Acta Met.*, 1967, vol. 15, p. 885.
5. A. S. Keh, Y. Nakada, and W. C. Leslie: in *Dislocaton Dynamics*, Rosenfield, Hahn, Bement, and Jaffee, eds., McGraw-Hill Publishers, 1968.
6. G. W. Ardley and A. H. Cottrell: *Proc. Roy. Soc.*, 1953, vol. 219A, p. 328.
7. G. F. Bolling: *Phil. Mag.*, 1959, vol. 4, p. 537.
8. B. Russel: *Phil. Mag.*, 1963, vol. 8, p. 615.
9. R. K. Ham and D. Jaffrey: *Phil. Mag.*, 1967, vol. 15, p. 247.
10. V. A. Phillips, A. J. Swain, and R. Eborall: *J. Inst. Metals*, 1952-53, vol. 81, p. 625.
11. N. R. Borch, L. A. Shepard, and J. E. Dorn: *Trans. ASM*, 1960, vol. 52, p. 494.
12. N. G. Turner and W. T. Roberts: *J. Less-Common Metals*, 1968, vol. 16, p. 37.
13. B. A. Wilcox and A. R. Rosenfield: *Mater. Sci. Eng.*, 1966, vol. 1, p. 201.
14. F. D. Rosi and F. O. Perkins: *Trans. ASM*, 1953, vol. 45, p. 972.
15. W. R. Kiessel and M. J. Sinnot: *AIME Trans.*, 1953, vol. 197, p. 331.
16. M. Nishihara, S. Yamamoto, and S. Ota: *Japan Cong. Test Mater.*, 1962, vol. 5, p. 103.
17. B. Ramaswami and G. B. Craig: *Trans. TMS-AIME*, 1967, vol. 239, p. 1226.
18. V. Ramachandran and R. E. Reed-Hill: *Met. Trans.*, 1970, vol. 1, p. 2105.
19. V. Fidleris: *Amer. Soc. Test. Mater., Spec. Tech. Publ.* 458, 1970, p. 1.
20. R. K. Ham: *Phil. Mag.*, 1961, vol. 6, p. 1183.
21. H. Scholl and W. Knorr: *Acta Met.*, 1961, vol. 9, p. 63.
22. H. L. Burghoff and C. H. Mathewson: *AIME Trans.*, 1945, vol. 143, p. 45.
23. L. A. Shepard and J. E. Dorn: *AIME Trans.*, 1956, vol. 206, p. 1229.
24. A. H. Cottrell: *Seminar on Relation of Properties to Microstructure*, Cleveland, 1953, p. 131, American Society for Metals, 1954.
25. J. P. Pemsler: *J. Electrochem. Soc.*, 1958, vol. 105, p. 315.
26. A. H. Cottrell and M. A. Jaswon: *Proc. Roy. Soc.*, 1949, vol. 199A, p. 104.
27. L. J. Cuddy: *Met. Trans.*, 1970, vol. 1, p. 395.
28. B. J. Brindley and J. T. Barnby: *Acta Met.*, 1968, vol. 16, p. 41.
29. A. Orlová, M. Pahutová, and J. Čadek: *Phil. Mag.*, 1972, vol. 25, p. 865.